

Characterization of Liquid Electrophotographic Toner Particles Using Non-Polar Electrical Field Flow Fractionation and MALLS

Dale D. Russell, Michael W. Hill and Martin Schimpf

Department of Chemistry, Boise State University, Boise, Idaho

Non-polar electrical field flow fractionation (Np-EFFF) has been demonstrated to separate electrophotographic toner particles suspended in hydrocarbon medium according to the ratio of their diffusivities and their electrophoretic mobilities. While electrophoretic mobility has long been recognized as critical to the behavior of liquid toner particles in a development gap, the role of diffusivity has largely been ignored. Toner particles move in the development gap as a function of both parameters, and as toner particle size is reduced to achieve improvements in print quality, diffusivity becomes increasingly important. We present a method of quantifying and predicting the behavior of toner particles in the development gap of a print engine. Particles eluting from the Np-EFFF channel at the same retention volume would be expected to exhibit similar development characteristics in a printer. Consequently, Np-EFFF retention volume data can be used to predict image development performance of liquid toner particles. Using this instrument with the multi-angle laser light scattering (MALLS) detector permits simultaneous determination of particle size, and particle size distribution. Although it is theoretically possible to determine other fundamental particle parameters from Np-EFFF data, it is used here to separate particles for further analysis down stream. In practical application, these instrumental capabilities allow screening of very small toner test batches, thus conserving time, expense, and the amount of waste generated.

Journal of Imaging Science and Technology 44: 433–441 (2000)

Introduction

Liquid electrophotography continues to offer the promise of outstanding print quality in an affordable desktop printer, provided some very real practical difficulties are overcome. Better understanding of the fundamental physics of particle movement in the development gap could suggest engineering approaches to resolving some of the current practical limitations of this important printing technology.

It has long been understood that print quality is strongly affected by the distributions of both size and electrophoretic mobility (μ) of the toner particles. Using Henry's equation for the electrophoretic mobility, we see that there is a dependence on both particle size and charge (ζ potential)¹.

$$\mu \propto \zeta \cdot f(Ka) \quad (1)$$

where a is the particle radius, K is the inverse of the Debye length, and where the function $f(Ka)$ varies from a value of "1" for small particles with a diffuse double layer, to a value of "3/2" for large particles with a compressed double layer. Thus, the electrophoretic mobility of a particle has first order dependence on charge (ζ potential) and a small dependence on size. Characterization of particle movement in response to an imposed field will include independent determination of at least

two out of these three parameters: electrophoretic mobility, size and charge. As particle size is reduced in order to optimize certain aspects of print quality, diffusivity of the particles increases. An increase in diffusivity means that particles will exhibit a greater tendency to move against a concentration gradient. In the case of particles impelled toward a photoconductor by an electrical field, this means smaller particles will be more likely than larger ones to undergo diffusion away from the photoconductor surface, and are therefore less likely to adhere to the photoconductor. The advantage of using smaller particles in the toner is thus partially nullified. Higher fields may have to be imposed to achieve comparable print quality. In this article we describe how non-polar electrical field flow fractionation (Np-EFFF) can be used to separate charged toner particles by the ratio of their diffusivities and electrophoretic mobilities, with in-line detection and analysis by laser light scattering to determine particle size and size distribution. This method characterizes toner particles as they move in both an electrical field and a flowing medium, and permits prediction of particle behavior in an electrophotographic development gap.

Background and Theory

EFFF is a sub-technique of a group of analytical separation techniques known as field flow fractionation (FFF) developed by Giddings.^{1,2} In all of the various FFF sub-techniques a well defined fluid velocity profile is established within a ribbon shaped channel. Separation is achieved through the interaction of the analyte with a field that is applied perpendicular to the flow direction (Fig. 1).

Original manuscript received February 8, 2000

©2000, IS&T—The Society for Imaging Science and Technology

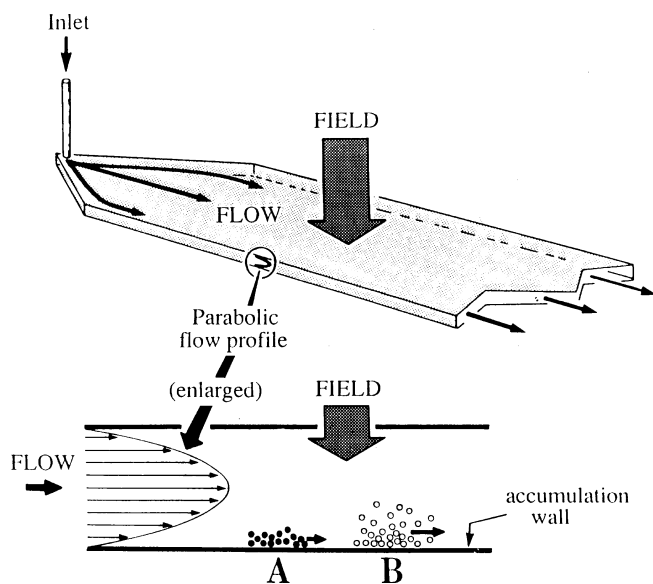


Figure 1. Schematic of a typical FFF channel. The enlargement shows the parabolic flow velocity profile. Sample “A” has a relatively particle interaction with respect to sample “B”.

Electrical FFF (EFFF) was first demonstrated in 1972 but failed to meet expectations due to its initial design.³ Design modifications that use the channel walls as electrodes, and work at relatively low applied fields, added significantly to the utility of this technique.⁴ In EFFF an electrostatic field is applied perpendicular to the flow of the carrier fluid, which until this work has been aqueous. At applied potentials as low as 1.7 V, electrolysis of the water can occur,⁵ as a result, the voltages must be kept low for aqueous solutions. In addition, when an electric field is applied across the channel, the strength of the electric field across the bulk of the channel is greatly reduced due to the electrical double layer effect.⁵ For these reasons, the method is not predicted to have much utility for aqueous particle dispersions such as water-based pigment inks.

An electrical double layer exists at all surfaces in contact with a fluid, including the surfaces of particles suspended in the carrier medium.¹ As it is used here, the term electrical double layer refers to the separation of charge that occurs at the interface between two phases. The electrical double layer is an electrostatic effect that is created by the interaction of the electrostatic field and any charge carriers or dipoles in solution. All charge carriers in solution will be attracted to the channel wall of opposite charge. The field will act to reorient any dipoles along the field lines and induce dipoles in non-polar molecules or particles. All of these conditions will act to reduce the effective field strength within the bulk of the solution. A finite double layer thickness will be established due to an interplay between the tendency of the charge on the channel walls to attract or repel charge carriers according to polarity, and the tendency of thermal processes to randomize them. In EFFF channels the flowing carrier also acts against the tendency of charge carriers to build up on the channel walls, thus reducing the electrical double layer effect.⁵

In polar solvents such as water, that can readily solvate charges, the electrical double layer effect will be very strong and this has been observed experimentally.^{5,6} In solutions with relatively high concentrations of small mobile charge carriers, the electrical double layer is com-

pressed into a very short distance, less than 100 Å.⁷ This means that an essentially field-free region exists only a few angstroms away from the surface of an electrode immersed in a conductive polar medium. In contrast, there is evidence that the electrical double layer extends a centimeter or more into fluids with low bulk conductivities (on the order of 100 pmhos or less).⁸ The diffuse nature of the electrical double layer in non-polar fluids makes it possible to generate an electrical field across a relatively large distance, such as the development gap in an electrophotographic printer, or the space between electrodes in an electrical field flow fractionation channel. The field does not have to be uniform to be successfully used to propel toner particles across the development gap of a printer. If the field is at least well defined, it can also be exploited for electrokinetic analysis of the fundamental characteristics of particles suspended in the medium.

FFF is similar to chromatography in that axial separation is achieved as an analyte flows through a channel. Unlike chromatography, separation is not accomplished through the interaction with a stationary phase. FFF is performed in an open channel with a well defined laminar flow profile as illustrated in Fig. 1. An external field is applied perpendicularly to the both the flow direction and the narrow dimension of the channel. A dynamic steady state is established between the two competing processes of the field induced transport, which tends to drive the analyte toward one of the channel walls (accumulation wall), and ordinary mass diffusion which tends to oppose accumulation at the wall. This steady state condition will confine the analyte to a region of space (zone) near the accumulation wall. Separation is achieved because different components of a mixture will interact more or less with the field, and/or have different diffusion rates, and this causes the different components to separate into different flow laminae. A dynamic steady state is established between the two competing processes of the field induced transport, which tends to drive the analyte toward one of the channel walls (accumulation wall), and ordinary mass diffusion which tends to oppose accumulation at the wall. This steady state condition will confine the analyte to a region of space (zone) near the accumulation wall. The velocity profile across the narrow dimension of the channel is nearly parabolic in shape,³ thus an analyte zone close to the wall will move slowly while a zone farther from the wall will move faster.

The expanded view of the channel cross section depicts two ideal analytes. Analyte “A” has a strong particle field interaction and/or a slow diffusion rate causing the population to be concentrated near the accumulation wall in slow moving laminae. Analyte “B” has a weaker particle field interaction and/or a faster diffusion rate causing its population to sample faster flowing laminae. Hence, population “B” moves through the channel with a greater average velocity and it elutes from the channel prior to population “A”.

The applied field drives the particles toward the accumulation wall, and a concentration gradient is established in response to the opposing motion of diffusion. An equilibrium distribution $c(x)$ is established when the field induced flux $J_F = Uc(x)$ is equal to the diffusive flux $J_D = D(dc(x)/dx)$, where U is the field induced velocity and D is the diffusion coefficient.

$$c = c_0 e^{(-xU/D)} \quad (2)$$

We can define $\ell = D/U$ as a characteristic zone thickness above the accumulation wall so Eq. 2 can be rewritten as,

$$c = c_0 e^{(-x/\ell)} \quad (2a)$$

where c_0 is the concentration at the accumulation wall.⁹ Note that this equation is valid as long as the particle size is small compared to the thickness of the accumulation zone. This is referred to as “normal mode” operation. When the particle size is comparable to or larger than the accumulation zone, this is referred to as “steric mode” of operation.¹⁰ Differences relative to the steric mode operation are discussed below.

The retention ratio, R , is defined as the ratio of the mean zone velocity to the mean carrier velocity. Given the concentration distribution above, if an infinite parallel plate model¹¹ is assumed, with a characteristic parabolic flow profile, we obtain the following analytical expression for the retention ratio,¹⁰

$$R = 6\lambda \cdot [\coth(2\lambda)^{-1} - 2\lambda] \quad (3)$$

where λ is the dimensionless retention parameter defined as ℓ/w , and w is the channel thickness. Experimentally the retention ratio is determined from the ratio of the void volume, V_0 , the elution volume of an unretained species, and the retention volume of the analyte, V_R .

$$R = \frac{V_0}{V_R} \quad (4)$$

The expression above for the retention ratio, as a function of λ is valid only if the particles are assumed to be point masses, i.e. particles whose size can be considered negligible compared to the accumulation zone thickness. When the particle size approaches that of the zone thickness, the expression given in Eq. 2 is no longer valid, and therefore neither is Eq. 3, and the so-called steric mode is encountered. In steric mode, the particles are essentially closely packed against the accumulation wall, as a result, the larger particles extend farther into the fast flowing region of the channel and will elute first. The smaller particles are also closely packed against the accumulation wall but because of their smaller size they do not extend as far into the faster flowing region and will elute after the larger particles. A modified retention equation for the steric mode is given as,¹²

$$R = 6 \cdot \left[\frac{a}{w} - \left(\frac{a}{w} \right)^2 \right] + 6\lambda \cdot \left(1 - \frac{2a}{w} \right) \cdot \left[\coth \frac{1-2a/w}{2\lambda} - \frac{2\lambda}{1-2a/w} \right] \quad (5)$$

where a is the particle radius. It can easily be shown that Eq. 5 reduces to give the same result as Eq. 3 at the limit of small radius.

EFFF

A charged particle in an electric field will experience a force that acts to attract the particle to the electrode of

opposite polarity. The force will be proportional to the electric field strength and to the net charge on the particle. The migration velocity, U , i.e. the velocity of the particle parallel to the field, will be directly related to the force on the particle and inversely related to the friction between the particle and the carrier,⁵

$$U = \left(\frac{Q}{f} \right) \cdot E \quad (6)$$

where Q is the charge on the particle, f is the frictional term and E is the electric field strength. The electrophoretic mobility μ , is defined as the ratio of the charge to the frictional drag, $\mu = Q/f$. The characteristic zone thickness can now be expressed in terms of the electrical parameters as,

$$\ell = \frac{D}{U} = \frac{Df}{QE} = \frac{D}{\mu E} \quad (7)$$

and the dimensionless retention parameter as,

$$\lambda = \frac{\ell}{w} = \frac{D}{\mu E w} \quad (8)$$

It can be shown that the retention ratio in EFFF is a function of the applied electric field as well as the particle's electrophoretic mobility and ordinary mass diffusion. λ can be determined from the ratio of V_0 to V_R . The experimental parameters w , channel thickness, and E , applied field strength, are controlled and known by the operator, but due to the double layer effect, the effective field E_{eff} , will be some fraction of E . Thus Eq. 8 should be written as a function of E_{eff} not E .

$$\lambda = \frac{\ell}{w} = \frac{D}{\mu E_{eff} w} = \frac{D}{\mu c E w} \quad (9)$$

where $E_{eff} = cE$. “ c ” is a constant that can be determined by calibration using a standard with known D and μ . Once E_{eff} has been established, Eq. 9 can be used to determine D , if μ is known, or to determine μ , if D is known. The calibration constant c will be system dependent, depending on channel thickness and carrier liquid.

Comparison of Np-EFFF to Other Methods of Toner Analysis:

This method has some advantages over other methods, and provides both confirming and complimentary information. One important difference is the fractionation capability inherent in all elution techniques. In most commercially available instruments intended for the analysis and characterization of non-polar suspensions, toner is analyzed in batch mode. This means that the data obtained for any parameter is an average value of that parameter for the whole dispersion. Examples include the electrophoretic sonic amplitude experiment (ESA), and most particle sizing instrumentation. For some instruments, a distribution of values may also be obtained, for example in many particle size analyzers such as the disk-centrifuge. In contrast, in Np-EFFF each sub-group is physically separated from others and elutes at a different times from the channel. Therefore the sub-groups may be further characterized as a sub-group, for example according to size. The use of the

MALLS detector permits characterization of size and size distribution on-line. If the individual sub-group fractions are collected as they elute, other sub-group parameters could be investigated off line, as desired.

A second advantage of the Np-EFFF instrument presented here lies in the design of the instrument to exploit the nature of the non-polar carrier medium. Most commercially available instruments marketed for analysis of charge or electrophoretic mobility are designed for analysis of aqueous (or at least polar) dispersions, with attachments or modifications to accommodate the special conditions of the non-polar dispersion. The instrument described here is the first system we are aware of designed specifically for non-polar dispersions, and which exploits these characteristics to advantage (as described above).

Taken together, these advantages yield direct information about liquid toners that is not available from other instruments. In Np-EFFF, the toner particles can be physically separated into sub-groups that elute at different times. Co-eluting particles have in common their ratio of μ and D , the parameters that determine their imaging behavior in the development gap. Each co-eluting group of particles is individually characterized with respect to its average ratio, and its distribution within this average ratio. This permits collection and individual characterization of each co-eluting group in order to determine the chemical and physical features of the group that give it a better or worse performance with respect to development. Once the optimum μ/D is determined for a given print engine, Np-EFFF permits rapid screening of toner formulations. For example, a toner formulation that yielded a single narrow peak from the Np-EFFF column at the optimum μ/D ratio would be expected to yield high quality images in development because all particles within the formulation exhibit the same charge/size characteristic, regardless of the distributions of either individual particle size or individual electrophoretic mobility. In contrast, a formulation could conceivably be very monodisperse with respect to size yet give a broad range of μ/D values. Such a formulation might be expected to yield poorer image development. Np-EFFF's ability to fractionate according to electrophoretic mobility and diffusivity is not shared by any commercially available instrument at this time.

Experimental

A schematic of the EFFF apparatus is shown in Fig. 1. The design employs a ribbon shaped channel that is obtained by sandwiching a thin, shaped, electrically insulating gasket between two parallel plate electrodes. The electrodes are insulated from the carrier liquid with a thin layer of polytetrafluoroethylene (PTFE) that prevents charge transfer processes from occurring across the dispersion/electrode boundary. Inlet and outlet ports at the apex at each end of the channel permit fluid flow through the channel. The channel dimensions are $125 \mu\text{m} \times 67 \text{cm} \times 1 \text{cm}$. Due to the high aspect ratio of the channel, a parabolic flow profile develops across the narrow dimension. This is shown in the blow-up in Fig. 1. An Alltech model 301 HPLC pump is used to pump the carrier solution through the channel, and an HP series 1050 UV detector is used in combination with a Wyatt Technology miniDAWN to detect and size the eluting particles. The typical fluid flow rate throughout the following experiments is 0.2 mL/min . A Rheodyne model 7725 seven port sample injection valve is used to inject typically a $20 \mu\text{L}$ sample into the channel. An HP model

33120A function generator is used to control and monitor the electrostatic potential across the channel.

Unlike a typical aqueous EFFF channel,^{5,6} the PTFE coated channel used here is electrically insulated from the external charging circuit. This was done intentionally in order to eliminate all electrochemical reactions across the channel boundary. An artifact of this insulating boundary is that it is now possible for an electrostatic charge to build up on the channel walls. In a system with a high charge carrier concentration, the electrostatic charge would be quickly dissipated. In our system, with a low charge carrier concentration, a static charge on the walls could last for minutes or hours. An electrostatically charged wall is easily detected by observing an elution profile with no applied field. If particle retention is observed, we conclude that the walls have acquired an electrostatic charge. In order to combat this problem, a sample is injected into the channel while a field with opposite polarity is applied. Although a small static charge may build up during the course of a single experiment, it is not allowed to build up over the course of multiple experiments.

The solvent used in all of this work is Norpar-12™ available from Exxon Corporation. This is a normal paraffinic hydrocarbon with average chain length of 12 carbons and a conductivity of $<0.1 \text{ pmho}$. The cell filled with this solvent behaves very much like a capacitor, and I/E calculations may be approximated using standard formulas. The carrier solution used is a 5000/1/1 mixture of Norpar with a non-ionic surfactant Triton N-42 and a zirconium metal soap respectively. The conductivity of this mixture was measured with a Scientifica model 627 conductivity meter and found to be 1.7 pmho/cm .

A solution of dodecane-soluble zirconium hexadecanoate (Hex-Cem™) is available from Mooney Chemical (Cleveland, OH). Dispersions of various pigments, including Sun Fast Blue 15:3, Sun Brite Yellow 83 and Sun Brite Maroon 63 are prepared in-house and used as electrophotographic toners. The pigments, obtained from Sun Chemical, Cleveland, OH, are homogenized into the carrier fluid along with a block co-polymeric dispersing agent and the zirconium soap charge director. This method of toner formulation is well known in the industry. Toners were characterized for average particle size and particle size distribution using Horiba LA-900 particle sizing instrument which is based on laser light scattering, and Brookhaven DCP-BI disk centrifuge particle sizing instrument.

Beta carotene, used as a void volume marker, is available at retail stores as a health food supplement.

Results and Discussion

EFFF permits separation of components in a mixture according to differences in the strength of the coupling between the electrostatic field and the respective components in the mixture. Particle retention is proportional to $D/\mu E$. If the coupling between the field and the particle is weak, or if the particle is a fast diffuser, then there is no measurable retention. The greater the particle field interaction or the slower the diffusion rate, the greater the retention. This is shown in Fig. 2. A mixture of beta carotene and yellow toner particles is separated due to differences in electrophoretic mobility and diffusion rate. The beta carotene is a small, highly soluble, uncharged molecule that is not retained by the field and elutes with the solvent front. Thus, it can be used to determine the channel void volume, i.e., the geo-

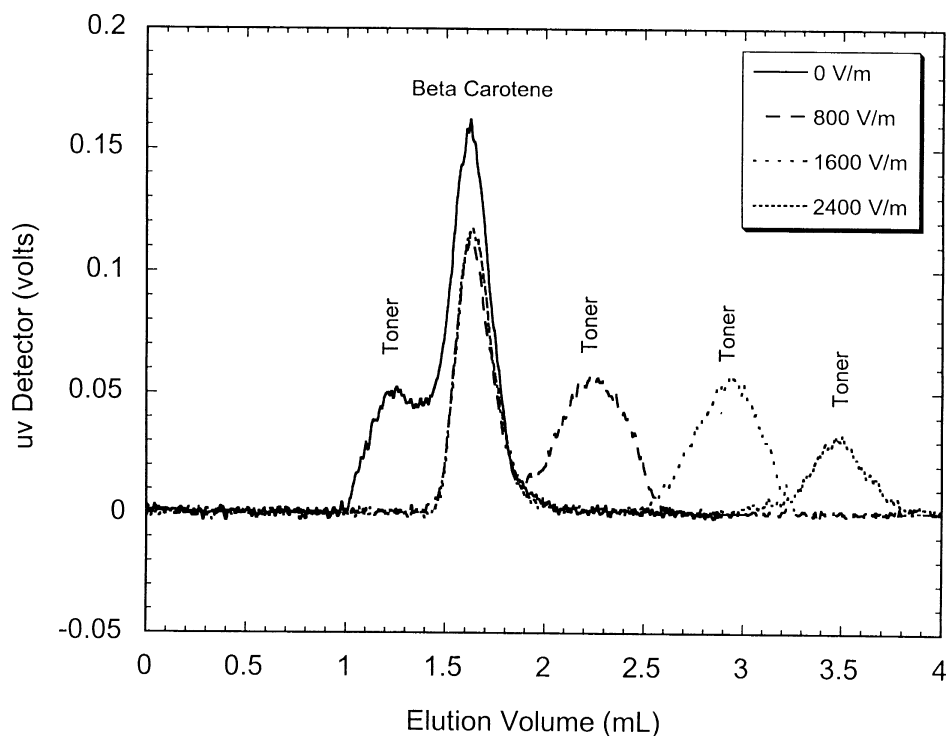


Figure 2. A mixture of beta carotene and yellow toner is separated due to differences in electrophoretic mobility and diffusion rate. The beta carotene always elutes at the void volume independent of field strength, while the yellow toner interacts with the field and is retained accordingly.

metric volume of the channel, or the volume of carrier required to elute an unretained species. The yellow toner particles are retained, and the retention volume can be seen to depend on the field strength. The beta carotene peak position is invariant with field strength and it is always observed at 1.63 mL. The geometric volume of the channel is calculated to be 1.56 mL, and the extra column volume is estimated to be approximately 70 μ L. Because the elution volume of an unretained species is the void volume (V_0) plus the extra column volume (V_{ex}), the beta carotene elution volume and the geometric volume are consistent.

With no external field one would expect that the toner would co-elute with the beta carotene. What is observed is that the toner elutes before the beta carotene (“pre-void” elution). This is consistent with observations of other researchers in the field.¹⁴ At present, there is no definitive explanation for this observed phenomenon. It may be assumed that the beta carotene is homogeneously distributed across the narrow dimension of the channel. Its elution volume is then that determined from the average fluid velocity through the channel. The conceptualization of how the toner can elute pre-void, is that the toner is not homogeneously distributed across the channel, but instead it is confined to laminae in the center of channel.¹³ If this is the case, then it will have a greater average velocity than the average fluid velocity through the channel. The confinement to the center could be due to repulsion of particles by the channel walls due to a relatively large difference in their electrochemical potentials.

The peak flow velocity in the center of the channel can be shown to be $3/2$ the average flow velocity.¹⁴ A species with a large diffusion coefficient will sample all flow lamina, and thus move with the average flow velocity of the carrier fluid. A species confined to the center lamina

of the channel will have a flow velocity that is up to $3/2$ the average flow velocity. This equates to a retention volume that is only $2/3$ that of the V_0 . In reference 14 it is shown that in a rectangular channel design such as an FFF channel, a sample that is confined to the center 10% of the channel will elute pre-void. And, the volume determined by the volume where the peak height is 86% of the maximum peak height on the leading edge of the peak, is $V_{ex} + 2/3 V_0$. The volume at 86% of the maximum peak height for the pre-void peak in Fig. 2, occurs at ~ 1.17 mL. With an extra column of 0.07 mL and a void volume of 1.56 mL, $2/3 V_0 = 1.04$, and $2/3 V_0 + V_{ex} = 1.11$. This is a difference of less than 5% between the observed value and that predicted for the pre-void peak assuming a distribution of particles within the center 10% of the channel thickness. The difference is consistent with a broader distribution than 10%. At present, we can conclude that, with no applied field, the toner particles are focused to the center region of the channel, but the mechanism for this is unclear.

Each of the three toners has been fractionated in the Np-EFFF channel and the mass distribution across the elution profile was determined using laser light scattering. Figures 3, 4, and 5 show the elution profile for the three different toner particles. Figures 3a, 4a, and 5a show the light scattering intensity at 90° , and Figs. 3b, 4b, and 5b show the UV absorption signal along with the R.M.S. radius as a function elution volume. The size separation power of Np-EFFF can be seen in these three figures. The smaller particles elute first and the larger particles follow. The size separation could be due to differences in both the electrophoretic mobility and diffusion, but because the size dependence of electrophoretic mobility is small,¹ it is most likely due to the size dependence of the diffusion coefficient (in Eq. 1 we see that $f(Ka)$ varies from 1 when $Ka = 0$, to 1.5 when $Ka = \infty$,

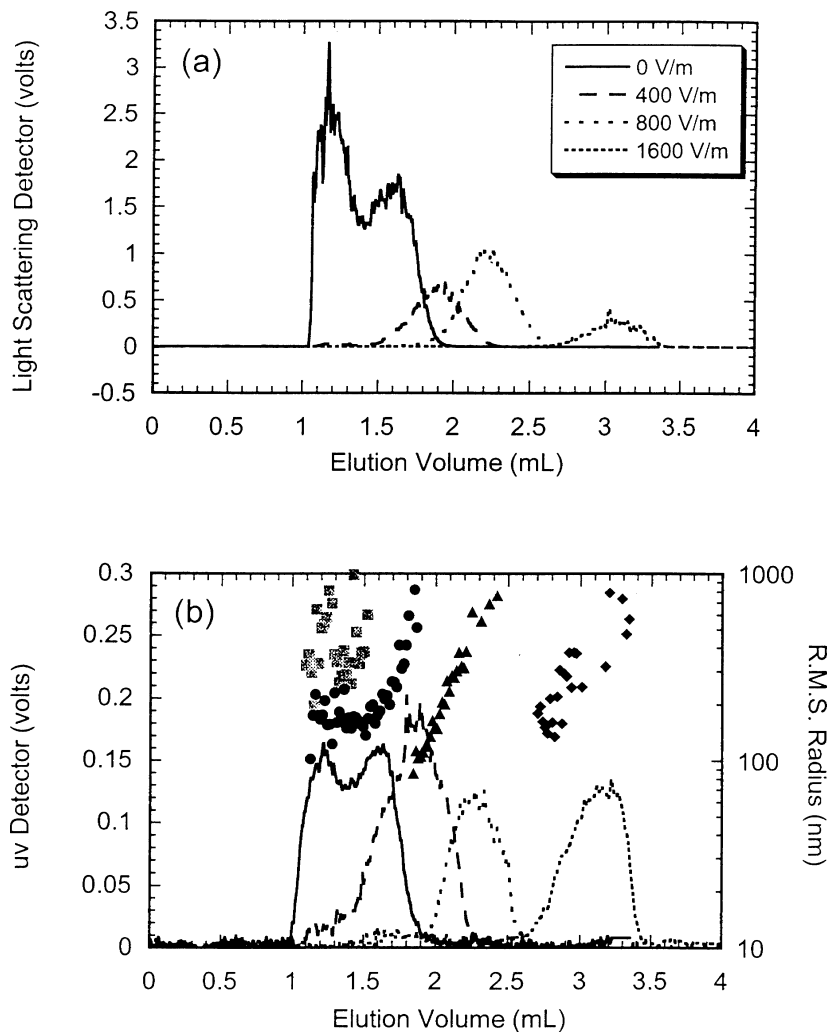


Figure 3. Elution profiles for yellow toner particles. UV absorbance at λ_{\max} for the yellow pigment, 450 nm. (a) Light scattering intensity versus elution volume for four different applied potentials. (b) UV absorption signal versus elution volume on the left axis and toner particle R.M.S. radius on the right axis. Solid gray squares = R.M.S. radius, no applied field; solid circles = 400 V/m; solid triangles = 800 V/m; solid diamonds = 1600 V/m.

while $D \propto 1/a$). The larger particles have a smaller coefficient of diffusion and they are less likely to diffuse away from the accumulation wall to counter the field driven migration. Because the larger particles are closer to the wall on average, they move in a slower flow lamina and elute from the channel after the smaller particles. The behavior of these particles in the Np-EFFF channel would also be expected to occur in the development gap of a print engine. The particle size distribution and concomitant distribution of diffusivities could impact on image quality, and also on the usable lifetime of the toner in the print cartridge, as larger particles are preferentially removed in the image development process.

Figures 3, 4, and 5 show consistently that with no applied field, there is no size separation for any of the three toners. This is predicted by theory. Because there is no size separation, small and large particles co-elute, and because the light scattering detector is more sensitive to the larger particles, the larger particles have greater weighting in the calculated particle size. Thus, with no applied field, i.e., no separation, the average particle size appears higher than the actual particle size.

A rather large distribution in particle size can be seen in these three figures. The average R.M.S. radius for the blue, maroon, and yellow toners is 139 ± 16 nm,

175 ± 47 nm, and 257 ± 49 nm respectively. If the toner particle is assumed to be a homogeneous sphere, then the hydrodynamic radius is related to the R.M.S. radius by

$$R_{RMS} = \sqrt{\frac{3}{5}a^2}$$

where “ a ” is the hydrodynamic radius.¹⁴ Using this relationship, the radius for the toner particles is 179 ± 21 nm, 226 ± 61 nm, and 332 ± 63 nm respectively. The nominal radius of the dye color centers of the blue, maroon, and yellow toners is 160 nm, 190 nm, and 270 nm respectively.

One hurdle in the development of the Np-EFFF with these toners, was the problem of particle flocculation on the channel walls. This problem is inherent to this toner system because the toner particles were designed to form a thin film on the photoconductor during the printing process. The two factors that had the greatest impact in reducing this problem for the Np-EFFF analysis were: 1) to coat the electrodes with a non-stick coating, PTFE, and 2) to have sufficient charge director in solution, favoring full charge on the particles.

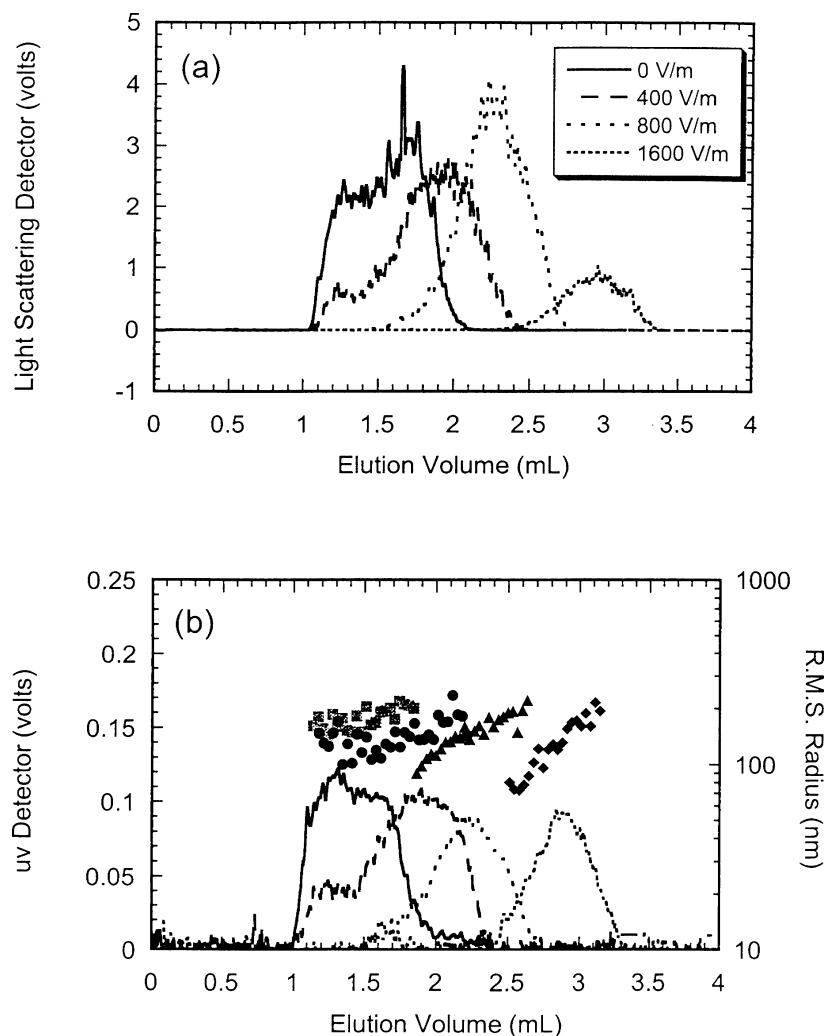


Figure 4. Elution profiles for the cyan (“blue”) toner particles. UV absorbance at λ_{\max} for cyan pigment, 600 nm. (a) Light scattering intensity versus elution volume for four different applied potentials. (b) UV absorption signal versus elution volume on the left axis and toner particle R.M.S. radius on the right axis. Solid gray squares = R.M.S. radius, no applied field; solid circles = 400 V/m; solid triangles = 800 V/m; solid diamonds = 1600 V/m.

Interactions between the particles and the channel walls still occur as field strength is increased, and this interaction can give us some insight into the flocculation process. The light scattering signal in Figs. 3a, 4a, and 5a shows a distinctive drop in intensity as the field strength is increased. Figures 3b and 4b show the UV absorbance of the pigment color center of the toner particles, but Fig. 5b is taken at a wavelength that shows the UV absorbance of free polymeric dispersing agent. From Fig. 5b we can see that the amount of free polymeric dispersing agent eluting from the channel increases when the amount of toner particles eluting decreases.

The extent of particle flocculation on the walls is a function of the applied field. With no applied field, there is little or no particle flocculation, the amount of free polymeric dispersing agent seen, with no applied field in Fig. 5b, is probably due to free dispersing agent present in the injected sample solution. Applying a field across the channel causes some of the toner particles to adhere to the accumulation wall, and the greater the field the greater the extent of this process. During the flocculation process the particles lose some of the polymeric dispersing agent. The polymeric dispersing agent

may be charged, but its molecules are expected to be small enough that its large diffusion constant prevents it from being retained significantly. This is why it comes out in the void volume and its retention does not change with increasing field strength.

For each of the three toners the retention can be seen to increase with an increase in the applied field strength. According to the theory, there should be a linear inverse relationship between the applied field and the retention parameter λ . This is indeed the case as shown in Fig. 6. In this figure we have plotted λ versus $1/E$ for the three different toners. It follows from Eq. 8, that the slope of this line is equivalent to $D/\mu cw$. “ c ” and “ w ” are system dependent parameters and “ D ” and “ μ ” are particle dependent parameters. For a given system, i.e., solvent and channel, “ c ” and “ w ” will remain constant and the slope of the line in Fig. 6 will vary due to the ratio D/μ . Channel width “ w ” is known but not the calibration constant “ c ”. Once “ c ” is determined by calibration with a known standard, the slope of this line can be used to determine the ratio D/μ . There are a number of ways to determine D independently. For example, it can be calculated by using the Stokes-Einstein equation with the particle hydrodynamic radius determined

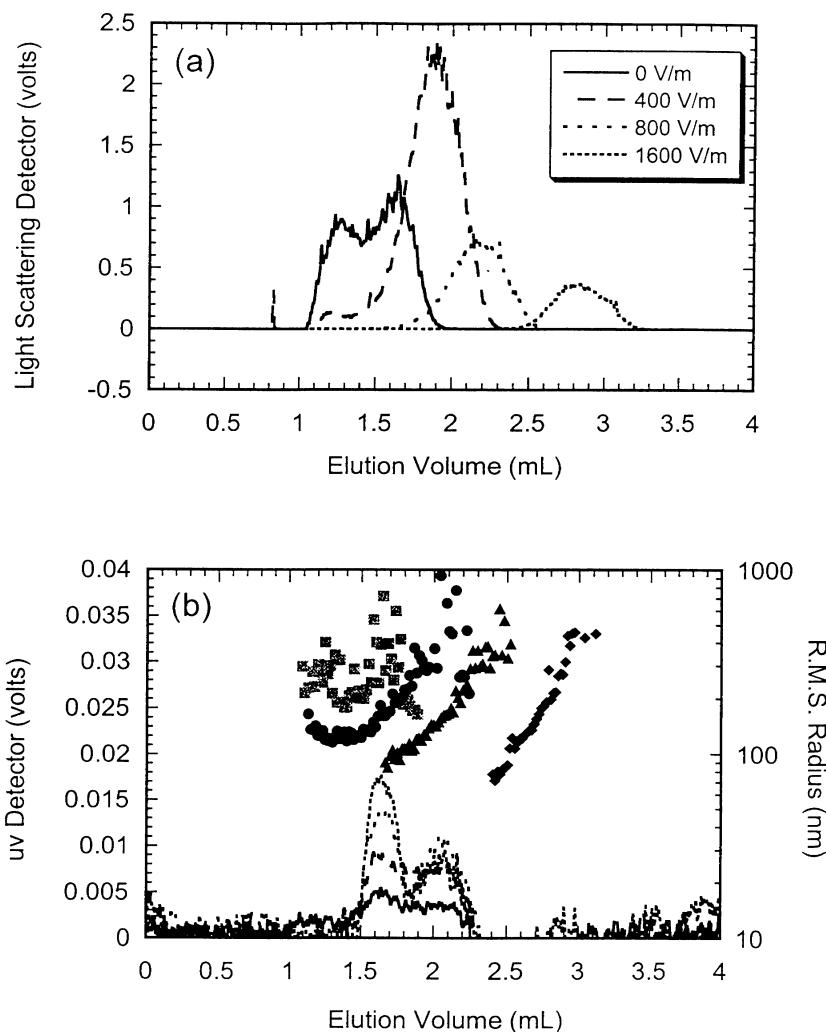


Figure 5. Elution profiles for the magenta (“maroon”) toner particles. UV absorbance at λ_{\max} for the polymeric dispersing agent, 250 nm. (a) Light scattering intensity versus elution volume for four different applied potentials. (b) UV absorption signal versus elution volume on the left axis and toner particle R.M.S. radius on the right axis. Solid gray squares = R.M.S. radius, no applied field; solid circles = 400 V/m; solid triangles = 800 V/m; solid diamonds = 1600 V/m.

by light scattering. Also D can be determined directly with dynamic light scattering.

One apparent inconsistency between theory and experiment is that a plot of λ versus $1/E$ should go through the origin. For all three toners, the line determined from this plot has a definite positive y-intercept. If the line were to have a negative intercept, there would be no theoretical explanation, but there is a plausible explanation for it to have a positive y-intercept. If the line goes through the origin, this means that at infinite field strength, λ equals zero, i.e., the retention volume is infinite. This is unreasonable unless the particles are physi-sorbed or chemi-sorbed onto the walls. As the field strength is increased the particle zone thickness is compressed closer to the accumulation wall. At infinite field strength, the particles are held tightly against the wall where now, steric exclusion alone defines the zone thickness. Thus, if the particles are not absorbed onto the accumulation wall, but the particle zone is partially compressed against the wall, a plot of λ versus $1/E$ will have a positive y-intercept.

The y-intercept gives the value of λ , i.e., the ratio of the sample zone thickness to the channel thickness,

when the applied field strength is infinite. When the data is extrapolated, the y-intercept is determined as $\lambda = 0.064$. This implies a mean zone thickness of 6.4% of the channel thickness. This value is larger than predicted for the amount of sample injected. Therefore, while this may be a factor in causing the positive y-intercept, there is obviously more to the problem. This question remains a topic for further study.

Conclusions

A new method for the characterization of liquid toner particles in non-polar carrier fluid has been demonstrated. Electrophotographic toner particles have been fractionated according to their diffusivities, sizes and electrophoretic mobilities in an Np-EFFF channel with Norpar-12 as the solvent. Particle retention and separation have been achieved with nominal electrostatic fields as low as 400 V/m, which is comparable to the field in the development gap of an electrophotographic print engine. Particle separation is achieved based on D/μ , and an in-line detector provides information on particle size and size distribution.

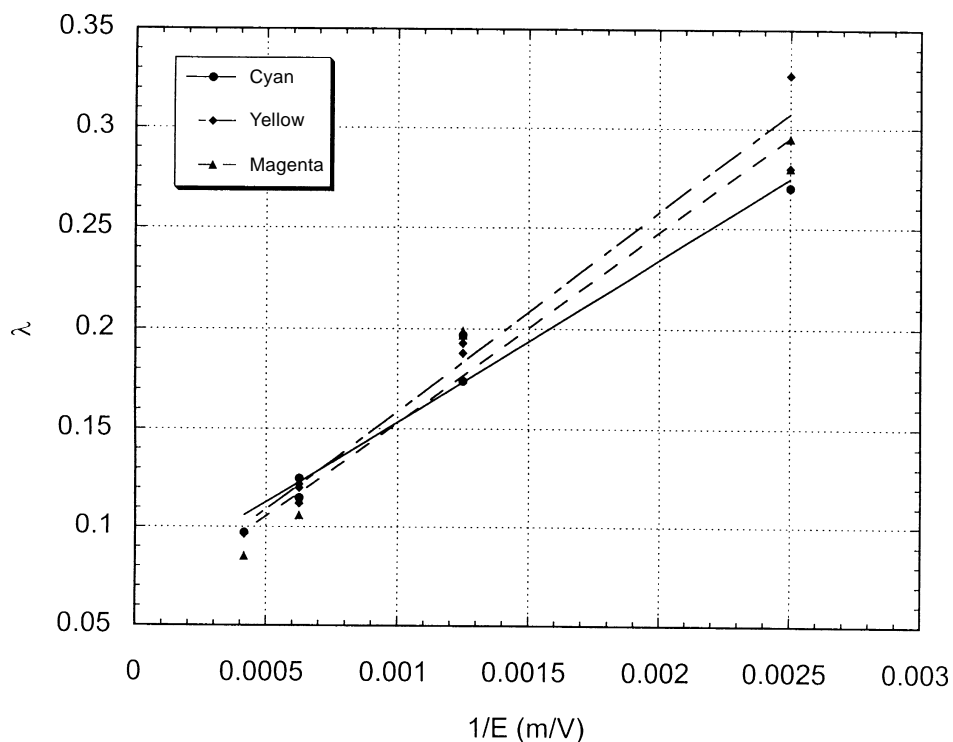


Figure 6. The plot of λ versus $1/E$ for the three toners shows linear relationship that agrees with the theory according to Eq. 8. These three toners were designed to give comparable image development on the photoconductor. This data predicts that they will.

This method will be useful for predicting behavior of toners in an electrophotographic print engine because it takes into account the impact of diffusivity on particle movement in a field. We are unaware of any other method that can do this simultaneously with a determination of size and electrophoretic mobility. With either a particle standard for electrophoretic mobility or an off-line method for determining particle diffusivity, this system can be calibrated to yield particle electrophoretic mobility. The results for a set of three toners was consistent with tests have printed image quality showing comparable image development under the same applied field. All of the toners used in this study have a broad size distribution that spans approximately one order of magnitude, as independently verified. We have shown that significant differences in behavior of these particles with size probably arise from the distribution of their diffusivities. We have shown that polymeric dispersing agent is released by the toner particles during the flocculation process. These observations and conclusions show the types of information that can be obtained with Np-EFFF for the analysis of large molecules or particles dispersed in non-polar solvents. \blacktriangle

References

1. J.C. Giddings, *Sep. Sci.* **1**, 123 (1966).
2. J.C. Giddings, *J. Chem. Phys.* **49**, 81 (1968).
3. K.D. Caldwell, L.F. Kesner, M.N. Myers, and J.C. Giddings, *Science* **176**, 296 (1972).
4. K.D. Caldwell and Y.S. Gao, *Anal. Chem.* **65**, 1764 (1993).
5. S.A. Palkar and M.R. Schure, *Anal. Chem.* **69**, 3223 (1997); S.A. Palkar and M.R. Schure, *Anal. Chem.* **69**, 3230 (1997).
6. M. Dunkel, N. Tri, R. Beckett, and K.D. Caldwell, *J. Micro. Sep.* **9**, 177 (1997).
7. A.J. Bard and L.R. Faulkner, *Electrochemical Methods Fundamentals and Applications*, John Wiley and Sons, New York, 1980, p. 506.
8. I.A. Bagotskaya and V.E. Kazarinov, *J. Electroanal. Chem.* **329**, 225 (1992); T. Gennett and M.J. Weaver, *J. Electroanal. Chem.* **186**, 179 (1985); N.M. Semenikhin and E.K. Zholkovskii, *Elektrokhimiya* **18**, 874 (1982); E.K. Zholkovskii and N.M. Semenikhin, *Elektrokhimiya* **18**, 1321 (1982); N.M. Semenikhin and E.K. Zholkovskii, *Elektrokhimiya* **18**, 691 (1982); N.A. Mishchuk and S.S. Dunkhin, *Elektrokhimiya* **49**, 276 (1987), (Translations of *Elektrokhimiya* are available from Plenum Publishing Co., NY, *Soviet Electrochemistry*).
9. M.E. Hovingh, G.H. Thompson and J.C. Giddings, *Anal. Chem.* **42**, 195 (1970).
10. J.C. Giddings, *Sep. Sci. Technol.* **13**, 241 (1978).
11. J. Happel and H. Brenner, *Low Reynolds Number Hydrodynamics*, Prentice-Hall, Englewood Cliffs, NJ, 1965, p. 34.
12. M.N. Myers and J.C. Giddings, *Anal. Chem.* **54**, 2284 (1982).
13. J.C. Giddings, P.S. Williams and M.A. Benincasa, *J. Chromatogr.* **627**, 23 (1992).
14. P.J. Wyatt, *Analytica Chimica Acta* **272**, 1 (1993).